Imaging and Quantitation of Cannabinoid CB₁ Receptors in Human and Monkey Brains Using ^{18}F-Labeled Inverse Agonist Radioligands

Garth E. Terry[1,2], Jussi Hirvonen[1], Jeih-San Liow[1], Sami S. Zoghbi[1], Robert Gladding[1], Johannes T. Tauscher[3], John M. Schaus[3], Lee Phebus[3], Christian C. Felder[3], Cheryl L. Morse[1], Sean R. Donohue[1], Victor W. Pike[1], Christer Halldin[2], and Robert B. Innis[1]

[1]Molecular Imaging Branch, National Institute of Mental Health, Bethesda, Maryland; [2]Psychiatry Section, Department of Clinical Neuroscience, Karolinska Institutet, Stockholm, Sweden; and [3]Lilly Research Laboratories, Lilly Corporate Center, Indianapolis, Indiana

We recently demonstrated that ^{11}C-MePPEP, a PET ligand for CB₁ receptors, has such high uptake in the human brain that it can be imaged for 210 min and that receptor density can be quantified as distribution volume (V_T) using the gold standard of compartmental modeling. However, ^{11}C-MePPEP had relatively poor retest and intersubject variabilities, which were likely caused by errors in the measurements of radioligand in plasma at low concentrations by 120 min. We sought to find an analog of ^{11}C-MePPEP that would provide more accurate plasma measurements. We evaluated several promising analogs in the monkey brain and chose the ^{18}F-di-deutero fluoromethoxy analog (^{18}F-FMPEP-d_2) to evaluate further in the human brain. **Methods:** ^{11}C-FMePPEP, ^{18}F-FEPEP, ^{18}F-FMPEP, and ^{18}F-FMPEP-d_2 were studied in 5 monkeys with 10 PET scans. We calculated V_T using compartmental modeling with serial measurements of unchanged parent radioligand in arterial plasma and radioactivity in the brain. Nonspecific binding was determined by administering a receptor-saturating dose of rimonabant, an inverse agonist at the CB₁ receptor. Nine healthy human subjects participated in 17 PET scans using ^{18}F-FMPEP-d_2, with 8 subjects having 2 PET scans to assess retest variability. To identify sources of error, we compared intersubject and retest variability of brain uptake, arterial plasma measurements, and V_T. **Results:** ^{18}F-FMPEP-d_2 had high uptake in the monkey brain, with greater than 80% specific binding, and yielded less radioactivity uptake in bone than did ^{18}F-FMPEP. High brain uptake with ^{18}F-FMPEP-d_2 was also observed in humans, in whom V_T was well identified within approximately 60 min. Retest variability of plasma measurements was good (16%); consequently, V_T had a good retest variability (14%), intersubject variability (26%), and intraclass correlation coefficient (0.89). V_T increased after 120 min, suggesting an accumulation of radiometabolites in the brain. Radioactivity accumulated in the skull throughout the entire scan but was thought to be an insignificant source of data contamination. **Conclusion:** Studies in monkeys facilitated our development and selection of ^{18}F-FMPEP-d_2, compared with ^{18}F-FMPEP, as a radioligand demonstrating high brain uptake, high percentage of specific binding, and reduced uptake in bone. Retest analysis in human subjects showed that ^{18}F-FMPEP-d_2 has greater precision and accuracy than ^{11}C-MePPEP, allowing smaller sample sizes to detect a significant difference between groups.

Key Words: positron emission tomography; brain imaging neuroimaging

The CB₁ receptor is associated with several neuropsychiatric disorders and is an active target for in vivo imaging development (*1*). We recently reported that the PET radioligand ^{11}C-MePPEP (Fig. 1) can image and quantify cannabinoid CB₁ receptors in the human brain (*2*). This radioligand has such high and stable uptake in the brain that it can be meaningfully imaged for 210 min after injection, and receptor density can be quantified using the gold standard of compartmental modeling with an arterial input function. Nevertheless, ^{11}C-MePPEP was limited by its short radioactive half-life (20.4 min), not because of low radioactivity in the brain but because of low radioactivity in arterial plasma by 120 min after injection. A PET radioligand using a radionuclide with a longer half-life (e.g., ^{18}F, 109.7 min) would provide for extended measurements from arterial plasma and hopefully allow more accurate quantitation of CB₁ receptors in the brain with compartmental modeling.

We recently synthesized three ^{18}F-labeled analogs of MePPEP: ^{18}F-FEPEP, ^{18}F-FMPEP, and ^{18}F-FMPEP-d_2 (Fig. 1) (*3*). The purposes of the present study were to compare the brain uptake of these 3 analogs in monkeys and evaluate the most promising candidate in humans. We

FIGURE 1. Structure of ^{11}C-MePPEP and its analogs.

V_T, which itself equals the ratio of $AUC_{0-\infty}$ of the concentration of radioactivity in the brain to $AUC_{0-\infty}$ of the concentration of parent radioligand in plasma.

found that the di-deutero fluoromethoxy analog ^{18}F-FMPEP-d_2 was the most promising candidate. Compared with MePPEP, FMPEP has a similar computed lipophilicity and similarly high selectivity for CB_1 versus CB_2 receptors but a slightly higher potency for CB_1 receptors (the functional inhibition constant [K_b] for displacement of methanandamide is 0.47 and 0.19 nM for MePPEP and FMPEP, respectively). Fluoromethoxy groups can be defluorinated in vivo, which leads to the uptake of ^{18}F-fluoride ion into bone. Radioactivity in the skull can contaminate the signal from the brain and artificially increase measurements. To reduce this potential problem, we substituted 2 deuteriums for the 2 hydrogens on the fluoromethoxy group. The carbon–deuterium bond is stronger than the carbon–hydrogen bonds (4), and breakage of this bond is thought to be an intermediate rate-determining step in defluorination, subject to primary isotope effect. This isotopic substitution has previously been reported to decrease the rate of defluorination in vivo successfully (5).

After evaluation in monkeys, we evaluated the ability of ^{18}F-FMPEP-d_2 to quantify CB_1 receptors in the healthy human brain using compartmental modeling. The outcome measure was total distribution volume (V_T), which equals the ratio at equilibrium of total radioactivity in the brain to the concentration of parent radioligand in plasma. Although V_T is the sum of specific and nondisplaceable uptake, studies in monkeys showed that greater than 85% of ^{11}C-MePPEP and ^{18}F-FMPEP-d_2 is specific binding (i.e., displaceable) in the brain (6). Our initial studies of ^{11}C-MePPEP in healthy human volunteers showed high intersubject variability of V_T, and we subsequently performed a retest study to identify the sources of variability (2). Assuming that both the clearance of ^{11}C-MePPEP from plasma and the density of CB_1 receptors in the brain were unchanged between the 2 scans, noise in the measurements of plasma radioactivity—particularly at late time points—was the likely cause of the high intersubject variability of V_T. Therefore, in the current study of ^{18}F-FMPEP-d_2, we measured the retest variability of 3 parameters critical to quantify CB_1 receptors in brain: clearance of the parent radioligand from plasma, assessed as the area under the curve of its concentration from time 0 to infinity ($AUC_{0-\infty}$); uptake of radioactivity in the brain at varying times; and

MATERIALS AND METHODS

Monkey Studies

Radioligand Preparation. ^{11}C-FMePPEP, ^{18}F-FEPEP, ^{18}F-FMPEP, and ^{18}F-FMPEP-d_2 were synthesized as previously described (3). The specific activities at the time of injection were 284 ± 115 GBq/μmol for ^{11}C-FMePPEP ($n = 2$), 150 ± 63 GBq/μmol for ^{18}F-FEPEP ($n = 4$), 140 ± 12 GBq/μmol for ^{18}F-FMPEP ($n = 2$), and 127 ± 93 GBq/μmol for ^{18}F-FMPEP-d_2 ($n = 2$). For all radioligands, the radiochemical purity was greater than 99%.

Monkey PET. Studies in monkeys were performed as described by Yasuno et al. (6), with the following deviations, in a total of 10 PET experiments in 5 male rhesus monkeys (weight, 11.6 ± 2.5 kg). Each radioligand was studied under baseline conditions and after CB_1 receptor blockade (rimonabant, 3 mg/kg intravenously) 30 min before radioligand injection. Baseline and receptor-blocked studies with the ^{18}F radioligands were performed at least 3 wk apart. Arterial blood samples were collected for all studies, except 1 baseline and 1 preblock study with ^{18}F-FEPEP. Monkeys receiving ^{18}F radioligands were scanned for 180 min and had additional arterial blood samples drawn at 150 and 180 min after radioligand injection. Specific binding was determined by (V_T baseline – V_T preblock)/V_T baseline × 100%.

Human Studies

Radioligand Preparation. ^{18}F-FMPEP-d_2 was prepared as previously described (3). The preparation is described in detail in our Investigational New Drug Application 100,898, submitted to the U.S. Food and Drug Administration (available at http://pdsp.med.unc.edu/snidd/). The radioligand was obtained in high radiochemical purity (>99%) and had a specific radioactivity at the time of injection of 111 ± 39 GBq/μmol ($n = 17$ batches).

Human Subjects. Nine healthy subjects (6 men and 3 women; mean age ± SD, 28 ± 8 y; mean body weight ± SD, 72 ± 16 kg) participated in baseline scans. Of these, 8 subjects (5 men and 3 women; mean age ± SD, 29 ± 7 y; mean body weight ± SD, 74 ± 16 kg) participated in retest scans. All subjects were free of current medical and psychiatric illness based on history, physical examination, electrocardiogram, urinalysis including drug screening, and blood tests including CBC and serum chemistries. The subjects' vital signs were recorded before ^{18}F-FMPEP-d_2 injection and at 15, 30, 60, 90, 120, 180, and 240 min after injection. Subjects returned for repeated urinalysis and blood tests about 24 h after the PET scan.

Human PET. After the injection of ^{18}F-FMPEP-d_2 (180 ± 6 MBq), PET images were acquired in 3-dimensional mode with an Advance camera (GE Healthcare) for 300 min. Scans were acquired continuously up to 120 min in 33 frames of increasing duration from 30 s to 5 min, followed by three 20-min scans of four 5-min frames each, at 160, 220, and 280 min after injection. Subjects participating in the retest studies had 15–245 d between scans (mean, 81 d; median, 60 d).

Measurement of ^{18}F-FMPEP-d_2 in Plasma. Blood samples (1.5 mL each) were drawn from the radial artery at 15-s intervals until 2 min, then at 3 and 5 min, followed by 3- to 4.5-mL samples at 10, 20, 30, 60, and 90 min; 4.5- to 9-mL samples at 120, 150, and

180 min; and 12-mL samples at 210, 240, and 270 min. The plasma time–activity curve was corrected for the fraction of unchanged radioligand by radio–high-performance liquid chromatography (HPLC) separation, as previously described (7).

The plasma free fraction of ^{18}F-FMPEP-d_2 was measured by ultrafiltration through Centrifree (Millipore) membrane filters (8). Free fractions were measured either 2 or 3 times for each sample on the same day of the PET scan. The formulation of ^{18}F-FMPEP-d_2 that was used to measure plasma free fraction did not contain polysorbate 80, which may affect plasma protein binding and whose presence would not be representative of in vivo conditions.

Image Analysis and Calculation of V_T Using Metabolite-Corrected Input Function

PET images were analyzed using coregistered MR images and a standardized template as previously described (2). Regional V_T and rate constants from standard 1- and 2-tissue-compartment models (9) were calculated using PMOD, version 2.95 (PMOD Technologies Ltd.) (10), with the arterial input function corrected for radiometabolites. Because of the uptake of radioactivity in the skull with ^{18}F-FMPEP-d_2, 4 regions were drawn on the coregistered MR images of each subject and applied to the PET images: combined left and right parietal bones, 9.3 ± 0.8 cm^3; occiput, 24.0 ± 1.5 cm^3; and clivus, 5.2 ± 1.6 cm^3.

To determine the minimal scanning time necessary to obtain stable values of V_T, we analyzed the PET data from each subject after removing variable durations of the terminal portion of the scan. We analyzed brain data of all subjects from 0–300 to 0–30 min, with 10-min decrements.

Statistical Analysis

Goodness of fit by the compartment models was determined as previously described (2) with F statistics (11), the Akaike information criterion (AIC) (12), and the model-selection criteria (MSC) (13). The most appropriate model is that with the smallest AIC and the largest MSC values. The identifiability of the kinetic variables was calculated as the SE, which reflects the diagonal of the covariance matrix (14). Identifiability was expressed as a percentage and equals the ratio of the SE to the rate constant itself. A lower percentage indicates better identifiability.

Group data are expressed as mean $\pm$ SD. Group analysis of brain data does not include white matter, because it does not contain significant amounts of CB$_1$ receptors. Intersubject variability was calculated as SD divided by the mean.

The retest variability and intraclass correlation coefficient (ICC) were calculated as described for ^{11}C-MePPEP in healthy subjects (2). To infer the relevance of a given ICC, we used a method to determine the statistical independence of 2 ICC values (15). We used the 2-way model to calculate the P value distinguishing ICC for V_T from that of brain uptake.

RESULTS

Monkey Studies

After the injection of ^{11}C-FMePPEP, radioactivity peaked in the brain at a standardized uptake value (SUV) of 3.3 by 30 min (Supplemental Fig. 1; supplemental materials are available online only at http://jnm.snmjournals.org) in a distribution moderately consistent with CB$_1$ receptor distribution (Supplemental Fig. 2). V_T was measured with a good identifiability (SE, 4%) and was stably measured within

about 90 min using a 2-compartment model. The specific binding was determined to be 73% from the receptor-blocking experiment (Supplemental Table 1). Because ^{11}C-FMePPEP had less brain uptake and specific binding than ^{11}C-MePPEP in monkeys (6), we did not study this radioligand further.

After injection of ^{18}F-FEPEP, peak radioactivity in the brain was an SUV of 2–3.5 at 15 min. V_T was measured with a good identifiability (SE, 3%) and stably measured within 90 min in most regions using a 2-compartment model. The cerebellum and pons showed an increasing V_T throughout the length of the scan. The specific binding was determined to be approximately 60% from the receptor-blocking experiment. SUV in the mandible reached 0.4–1.0 immediately after injection and remained the same for the duration of the scan (Supplemental Fig. 2D).

After injection of ^{18}F-FMPEP, peak SUV in the brain was 5–6.5 at 20 min. V_T was measured with a good identifiability (SE, 2%) and stably measured within about 90 min using a 2-compartment model. The cerebellum and pons showed an increasing V_T throughout the length of the scan. The specific binding was determined to be approximately 90% from the receptor-blocking experiment. SUV in the mandible reached approximately 1.4 within 10 min and increased to 3.1 by the end of the 180-min scan.

After injection of ^{18}F-FMPEP-d_2, SUV peaked in the brain at 4.5–6.5 by 20 min. V_T was measured with a good identifiability (SE, ~2%) and stably measured within about 90 min. The cerebellum, pons, and medial temporal cortex showed an increasing V_T throughout the length of the scan. The specific binding was determined to be 80%−90% from the receptor-blocking experiment. Radioactivity concentration in the mandible reached an SUV of approximately 1.3 within 10 min and increased to 2.0 by the end of the 180-min scan.

We selected the deuterated analog ^{18}F-FMPEP-d_2 for study in human subjects because it had high brain uptake, about one third less uptake of radioactivity in bone than the nondeuterated ^{18}F-FMPEP, and V_T that was well and stably identified.

Human Studies

Pharmacologic Effects. ^{18}F-FMPEP-d_2 caused no pharmacologic effects based on subjective reports, electrocardiogram, blood pressure, pulse, and respiration rate. In addition, no effects were noted in any of the blood and urine tests acquired about 24 h after radioligand injection. The injected radioactivity of ^{18}F-FMPEP-d_2 was 180 ± 6 MBq, which corresponded to 1.9 ± 0.8 nmol of FMPEP-d_2 ($n = 17$ injections in 9 subjects). Thus, an uptake of 4 SUV in the brain would correspond to a receptor occupancy of 0.06%, assuming the maximum number of binding sites is 1.81 pmol/mg of protein in the brain (16), that 10% of brain is protein, and that all ^{18}F-FMPEP-d_2 in the brain was bound to CB$_1$ receptors.

Radioactivity in Brain and Skull

After the injection of ^{18}F-FMPEP-d_2, all subjects showed high concentrations of radioactivity in the brain, consistent

with the distribution of CB_1 receptors (*17*), which decreased slowly over time. Radioactivity in the brain peaked by approximately 30 min and was approximately 3.2 SUV for all areas of the neocortex (Figs. 2 and 3A). Areas with high CB_1 receptor density (e.g., putamen) had an even greater concentration of radioactivity, peaking over 4.0 SUV in most subjects. Radioactivity in the brain decreased slowly, remaining within approximately 85% of the peak by 2 h and within approximately 60% of the peak by 5 h. We averaged radioactivity concentration from 20 to 60 min after injection to represent brain uptake (brain uptake$_{20-60}$; Supplemental Table 3).

Two regions of the brain consistently demonstrated less uptake of radioactivity than other regions. The first region, pons, had a peak SUV of approximately 2.4 within 8 min. After the peak, washout of radioactivity from the pons was 1.5–2 times faster than from other regions at 60–120 min after injection. The second region, white matter, typically peaked at an SUV of approximately 1.2 about 15 min after injection and remained nearly constant until the end of the scan, with minimal washout of radioactivity.

The skull had a significant uptake of radioactivity, which could reflect bone or marrow (Fig. 3B). Among regions of the skull, the clivus, which contains significant amounts of marrow, had the greatest uptake of radioactivity, suggesting that marrow more avidly takes up ^{18}F-FMPEP-d_2 or its radiometabolites.

Plasma Analysis

The concentration of ^{18}F-FMPEP-d_2 in arterial plasma peaked at 1–2 min and then rapidly declined because of
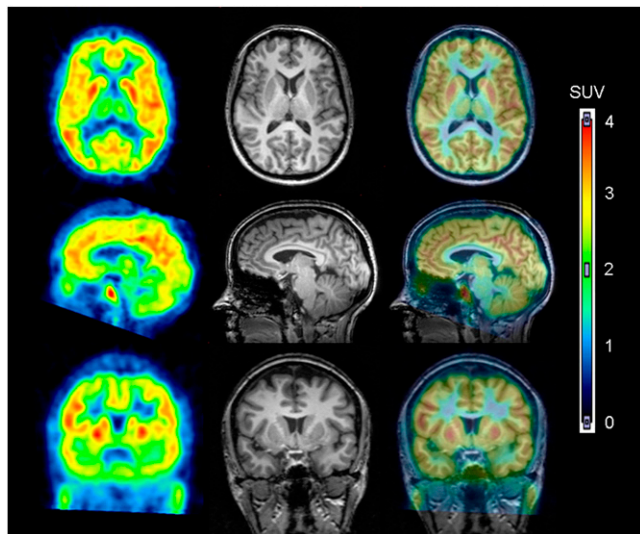

FIGURE 3. Time–activity curves of ^{18}F-FMPEP-d_2 in brain from single subject scanned for 300 min. (A) Decay-corrected measurements from putamen (■), prefrontal cortex (□), cerebellum (●), pons (○), and white matter (×) were fitted with unconstrained 2-tissue-compartment model (–). Putamen was consistently region of highest brain uptake. White matter was consistently region of lowest brain uptake, followed by pons. (B) Decay-corrected measurements from same subject demonstrate uptake of radioactivity in clivus (◆), occiput (◇), and parietal bones (▲). Concentration (Conc) is expressed as SUV, which normalizes for injected activity and body weight.

FIGURE 2. ^{18}F-FMPEP-d_2 in human brain. PET images from 30 to 60 min after injection of ^{18}F-FMPEP-d_2 were averaged (left column) and coregistered to subject's MR images (middle column). PET and MR images are overlaid in right column.
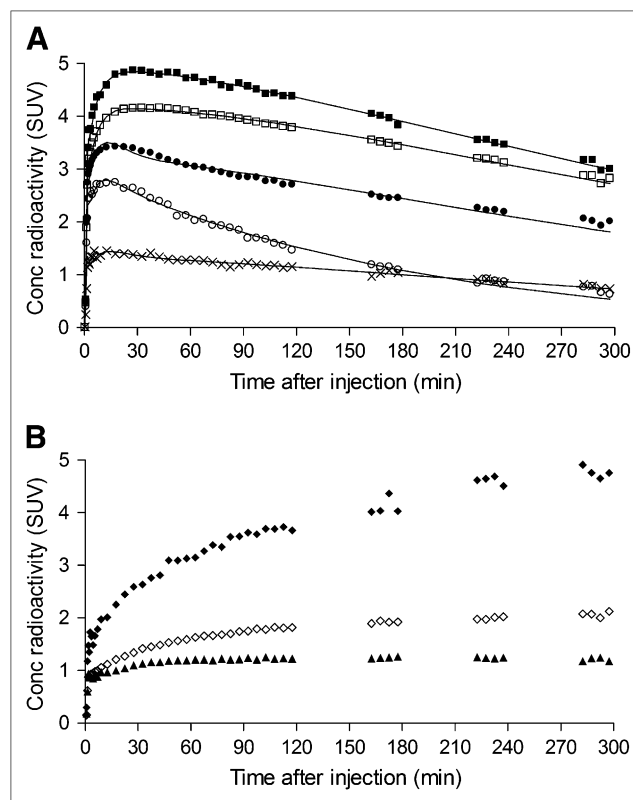
distribution in the body, followed by a slow terminal phase of elimination. To quantify the exposure of the brain to ^{18}F-FMPEP-d_2, we fitted the concentration of ^{18}F-FMPEP-d_2 after its peak to a triexponential curve (Fig. 4A). Of the 3 associated half-lives, the first 2 (~0.4 and 5.7 min) largely reflected distribution and the last (~82 min) reflected elimination (i.e., metabolism and excretion). However, the 3 components accounted for nearly equal portions of the total $AUC_{0-\infty}$: approximately 18%, 28%, and 33%. The portion before the peak accounted for approximately 20% of the $AUC_{0-\infty}$. The concentration of ^{18}F-FMPEP-d_2 in the plasma of some subjects remained the same or slightly increased during the 2 later imaging intervals (150–180 and 210–240 min) but declined during the rest intervals (120–150, 180–210, and 240–270 min). During the rest intervals, subjects arose from the camera and walked around, suggesting that the shifting of fluid in the body may have mobilized and redistributed ^{18}F-FMPEP-d_2.
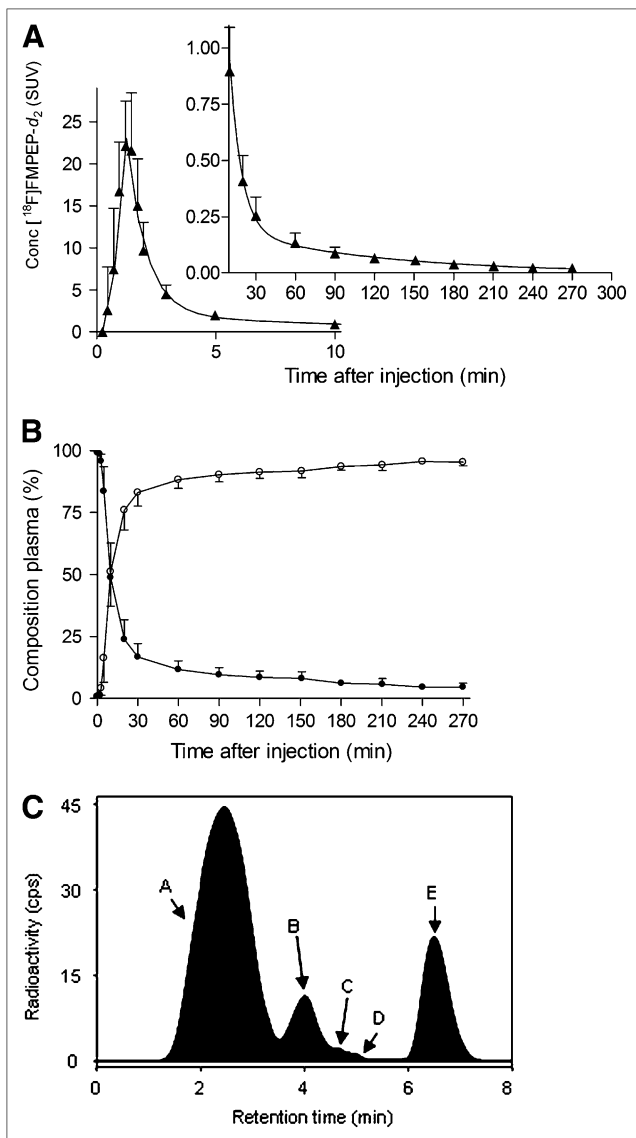
FIGURE 4. Concentration of ^{18}F-FMPEP-d_2 and its percentage composition in arterial plasma. (A) Average concentration of ^{18}F-FMPEP-d_2 in arterial plasma from 9 subjects is plotted over time after injection. Data after peak (~1 min) were fitted to triexponential curve (—). Symbols (▲) and error bars represent mean and SD, respectively. (B) Percentage composition of parent radioligand (●) and radiometabolites (○) in arterial plasma from 9 subjects are plotted over time after injection. After 60 min, ^{18}F-FMPEP-d_2 accounted for at least 11% of radioactivity in arterial plasma. (C) This radiochromatogram illustrates plasma composition from 1 subject, 30 min after injection of ^{18}F-FMPEP-d_2. Radioactivity was measured in counts per second (cps). Peaks are labeled with increasing lipophilicity from A to E. Peak E represents ^{18}F-FMPEP-d_2. Conc = concentration.

Several radiometabolites of ^{18}F-FMPEP-d_2 appeared in plasma (Figs. 4B and 4C). The main radiometabolite eluted earlier than ^{18}F-FMPEP-d_2 on reversed-phase HPLC and was presumably less lipophilic than the parent compound. The concentration of this radiometabolite peaked within 60

min and minimally declined for the remainder of the scan. Other radiometabolites were detected throughout the scan in varying concentrations and with various elution times on HPLC. After 60 min, ^{18}F-FMPEP-d_2 constituted only 11% of total radioactivity in plasma and declined thereafter.

The free fraction of ^{18}F-FMPEP-d_2 in plasma (f_P) was low. The average f_P was 0.63% ± 0.33% in 9 subjects, with an SD of 0.01% for repeated sample measurements. The f_P had a retest variability of 50% for 8 subjects.

Optimum Model and Scan Length for Kinetic Analysis

After 300 min of scanning, the unconstrained 2-compartment model provided a significantly better fit of the data in all subjects than did the 1-tissue-compartment model, consistent with the presence of both specific and nonspecific binding in the brain. Although the 1-tissue model estimated K_1, k_2, and V_T with reasonable identifiability (SE, 1%−6%), the curves significantly deviated from the measured brain data, especially in regions with low CB_1 receptor density. Compared with the 1-tissue model, the 2-tissue model had a statistically better fit to measured data by F test ($P < 0.05$), lower AIC scores (192 vs. 285, on average), and higher MSC scores (4.4 vs. 2.3, on average) for all brain regions.

For the 2-tissue-compartment model, we assessed the utility of constraining nondisplaceable uptake ($V_{ND} = K_1/k_2$) to a single value determined from all regions except white matter. When compared by F test, the unconstrained model fitted the data significantly better than did the constrained model in most regions, and the AIC and MSC scores favored the unconstrained model. For these reasons, we used the unconstrained 2-tissue-compartment model for additional analyses.

To determine the minimal scanning time necessary to obtain stable values of V_T, we calculated V_T and its identifiability using increasingly truncated durations of brain data. V_T was stably identified between 60 and 120 min, whereas its identifiability was best (i.e., SE was lowest) between 120 and 300 min (Fig. 5A). V_T gradually increased after 120 min, and regions closer to the skull increased more after 120 min than those in the center of the brain. Nevertheless, V_T increased in all brain regions after 120 min, which was consistent with the accumulation of radiometabolites in the brain. Therefore, we chose 120 min of scan data to determine V_T, because V_T was stably identified between 60 and 120 min, its identifiability was good, and additional scan durations would have greater contamination from radiometabolites. We confirmed that the 2-tissue-compartment model was superior to the 1-tissue-compartment model after 120 min of data based on the same criteria described above.

Kinetic Analysis and Retest Variability Based on 120 min of Scan Data

The value of K_1 in all regions except white matter ranged from 0.08 to 0.12 mL·cm^{-3}·min^{-1}, with an average of 0.10 mL·cm^{-3}·min^{-1} (Supplemental Table 2). Assuming that
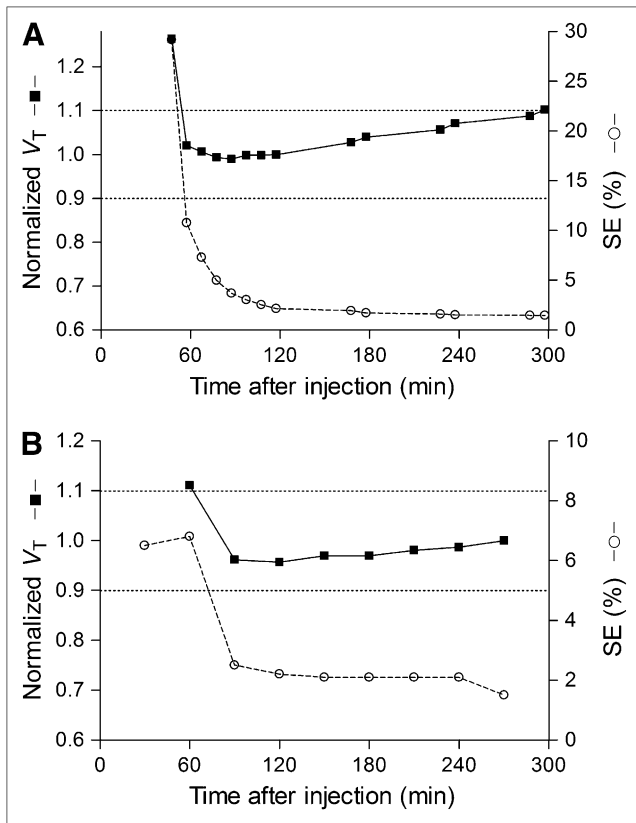
FIGURE 5. V_T of putamen and its identifiability as function of duration of image acquisition (A) and plasma measurements (B). V_T (■) was calculated using unconstrained 2-tissue-compartment model. Values were normalized to that determined from 120 min of imaging and are plotted with y-axis on left. Corresponding SE (○), which is inversely proportional to identifiability, is plotted with y-axis on right. Points represent average of 9 subjects. (A) Length of image acquisition was varied from 0–30 to 0–300 min, but entire input function (0–270 min) was used for all calculations. V_T was stably identified between 60 and 120 min but gradually increased thereafter. (B) Length of plasma input function was varied from 0–270 to 0–60 min, but initial 120 min of image acquisitions were used for all calculations. V_T was stably identified with as little as initial 90 min of plasma data.

cerebral blood flow is approximately 0.5 mL·cm^{-3}·min^{-1}, the extraction fraction (extraction = K_1/flow) of ^{18}F-FMPEP-d_2 from plasma to brain was approximately 20%. The value of k_2 in all regions except white matter ranged from 0.04 to 0.06 min^{-1}, with an average of approximately 0.06 min^{-1}. Thus, the value of nondisplaceable V_T (V_{ND} = K_1/k_2) was approximately 2.0 mL·cm^{-3}. The value of k_3, which is defined as $k_{on}·B_{max}·f_{ND}$, ranged from 0.085 to 0.143 min^{-1}, with an average value of approximately 0.112 min^{-1}. The value of k_4, which is proportional to the dissociation rate constant from the specific compartment, was low and ranged from 0.010 to 0.027 min^{-1}, with an average of approximately 0.018 min^{-1}. Finally, the estimated ratio of specific to nondisplaceable uptake (BP_{ND} = k_3/k_4) was approximately 7.3 in the healthy human brain.

Retest variability for ^{18}F-FMPEP-d_2 was moderate to good (Supplemental Table 3). The mean retest variability of brain uptake$_{20–60}$ and V_T was 16% and 14%, respectively. However, the ICC of V_T (0.89) was significantly better than that of brain uptake (0.39, $P < 0.03$). Finally, the retest variability of the plasma measurements alone was approximately 16%, as assessed by AUC$_{0-\infty}$.

The intersubject variability for V_T of ^{18}F-FMPEP-d_2 was moderate (~26%; Supplemental Table 2) and was greater than both the retest variability of ^{18}F-FMPEP-d_2 and the intersubject variability reported for other radioligands (10%−20%). The intersubject variability was lower for brain uptake$_{20–60}$ (~14%) than for V_T. The intersubject variability of the plasma measurements was also good, 20%, assessed as AUC$_{0-\infty}$.

The intersubject variability of V_T might have been affected by variations in the plasma free fraction of ^{18}F-FMPEP-d_2. However, the intersubject variability of V_T/f_P in all 8 brain regions of the 9 subjects scanned for 120 min was actually higher than that of V_T and ranged from 40% to 60%. The retest variability of V_T/f_P was also higher, again ranging from 40% to 60%, indicating that V_T/f_P has less precision than did V_T alone. Indeed, the retest variability of free fraction itself was approximately 50%. Thus, correction of V_T for individual values of plasma protein binding increased intersubject and retest variability and was likely a source of noise to the data.

To determine the minimal length of blood sampling required to measure V_T, we truncated the plasma data in a manner similar to the brain data (Fig. 5B). When plasma data were truncated from 270 to 120 min, plasma AUC$_{0-\infty}$ changed by only approximately 4% and V_T changed by only approximately 4%. Thus, plasma AUC$_{0-\infty}$ and V_T were well identified with this initial 120 min of plasma data.

Can Brain Uptake Substitute for V_T?

Brain uptake not corrected for plasma measurements has been used with another radioligand to measure CB$_1$ receptor availability in the human brain (18,19). With ^{11}C-MePPEP, we found that the intersubject variability and retest variability of brain uptake was much better than that of V_T. In contrast, brain uptake and V_T for ^{18}F-FMPEP-d_2 showed similar intersubject variability and retest variability. Similar to ^{11}C-MePPEP, we sought to determine whether brain uptake by itself would be a reasonably accurate surrogate for V_T and thereby avoid plasma measurements. We simulated increased and decreased receptor densities by corresponding changes in k_3. We used the average input function and rate constants for prefrontal cortex from the 9 subjects scanned for 120 min. Brain uptake was calculated for 4 time intervals: 20–60, 90–120, 280–300, and 0–300 min.

Brain uptake for all time intervals except 280–300 min followed the pattern of increasing or decreasing receptor density but underestimated the changes (Fig. 6). For example, a 50% increase in receptor density yielded
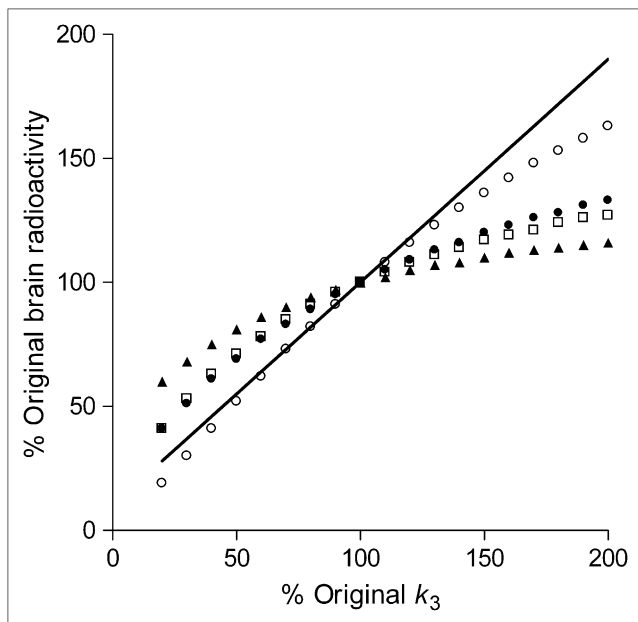
FIGURE 6. Simulated changes in brain uptake with variations of receptor density. Average individual kinetic parameters from prefrontal cortex were used to simulate expected changes in brain uptake at 280–300 (○), 0–300 (●), 90–120 (□), and (▲) 20–60 min. Changes in receptor density were simulated by varying value of k_3 from its mean value (set at 100% on x-axis). As expected, value of V_T (shown by line that has y-intercept equal to K_1/k_2) is directly proportional to changes in k_3.

a 10%−20% increase only of brain uptake during the time intervals 20–60, 90–120, and 0–300 min, whereas V_T increased by 45%. V_T includes both specific and non-displaceable uptake; thus, a 50% increase of k_3 and specific binding causes a 45% increase only of V_T. In addition, a 50% decrease in receptor density yielded a 19%−31% decrease only of brain uptake during these 3 time intervals, whereas V_T decreased by 45%. For simulations of brain uptake from 280 to 300 min, a 50% increase in receptor density yielded a 36% increase of brain uptake, whereas a 50% decrease in receptor density yielded a 48% decrease of brain uptake. This suggests that brain uptake$_{280–300}$ might accurately predict changes in receptor density. However, these simulations were performed with kinetic parameters attained after 120 min; later values of brain uptake may be contaminated by radiometabolites or radioactivity accumulating in the skull, decreasing the accuracy of these measurements.

We also calculated the expected number of subjects needed to detect these simulated outcome measurements. Estimation of sample sizes for a 2-tailed t test assumed $\alpha = 0.05$ (probability of type I error) and $\beta = 0.20$ (probability of type II error, that is, power of 80%). Intersubject variability from our measurements from 9 subjects was used to estimate the pooled SD of the 2 outcome measures: brain uptake and V_T. For a 50% increase of receptor density,

39 subjects would be required for brain uptake$_{20–60}$ versus 7 subjects for V_T. Additionally, for a 50% decrease of receptor density, 12 subjects would be required for brain uptake$_{20–60}$ versus 7 subjects for V_T.

DISCUSSION

This initial evaluation of ^{18}F-FMPEP-d_2 in healthy human subjects demonstrated that cannabinoid CB$_1$ receptors in the brain can be measured as V_T with good identifiability and precision and low retest variability. We recommend scanning for 60–120 min, with intermittent sampling of arterial blood to measure the parent radioligand in plasma. Scanning for more than 120 min is problematic for 2 reasons. First, the apparent value of V_T gradually increased during the interval from 120 to 300 min, suggesting that radiometabolites were accumulating in the brain. Second, radioactivity significantly accumulated in the skull during this same period, and spillover of activity would have contaminated measurements in adjacent brain. ^{18}F-FMPEP-d_2 is superior to ^{11}C-MePPEP largely because the longer-lived radioactivity permits greater accuracy and reproducibility of measurements, particularly for those from plasma. Finally, measurements of brain uptake alone, compared with V_T, are inaccurate. Brain uptake underestimates changes in receptor density and requires larger sample sizes than V_T to detect significant differences between groups.

Accumulation of Radioactivity in Skull

We compared three ^{18}F-labeled analogs in monkeys and selected ^{18}F-FMPEP-d_2 to study in humans because it had high uptake in the brain and one third less uptake of radioactivity in the skull than ^{18}F-FMPEP. Skull uptake can reflect in vivo defluorination and subsequent accumulation of ^{18}F-fluoride ion in bone. Despite our use of a dideuterated analog to decrease defluorination, ^{18}F-FMPEP-d_2 did yield substantial radioactivity uptake in the human skull, especially during the period from 120 to 300 min. We do not know whether the uptake in skull was in bone versus marrow or whether it was due to parent radioligand or radiometabolite. Nevertheless, to what extent did accumulation in the skull before 120 min confound measurements of V_T? To answer this question, we simulated the spillover based on resolution of the camera and the distance between skull and adjacent brain regions. We used conservative assumptions that would tend to overestimate spillover. Specifically, we assumed that the images had a resolution of 10 mm in full width at half maximum, that the cerebral cortical region was 10 mm wide, that the skull was 8 mm thick, that skull and cortex were separated by 5 mm, and that SUV was 2.4 in cortex and 1.7 in bone, which reflect measured values at 120 min. Using these conservative parameters, we estimated that radioactivity from the skull constituted only about 2% of measurements in adjacent cortex. Thus, contamination of neocortical activity from that in skull was negligible during the initial 120 min,

which itself was adequate to provide well and stably identified values of V_T.

Comparison of ^{18}F-FMPEP-d_2 to ^{11}C-MePPEP

The brain uptake of ^{18}F-FMPEP-d_2 and ^{11}C-MePPEP are fairly similar in the human brain (Supplemental Table 4). High and prolonged uptake allows ^{11}C-MePPEP to provide useful measures of brain radioactivity for 210 min, which we extended using the longer radioactive half-life with ^{18}F-FMPEP-d_2. ^{18}F-FMPEP-d_2 also tended to peak earlier and wash out faster than ^{11}C-MePPEP. Perhaps the most important difference between the 2 radioligands is the lower accuracy of plasma measurements for ^{11}C-MePPEP than for ^{18}F-FMPEP-d_2. For example, the retest variability of plasma $AUC_{0-\infty}$ was 58% for ^{11}C-MePPEP and 16% for ^{18}F-FMPEP-d_2. The relatively high retest variability of plasma $AUC_{0-\infty}$ for ^{11}C-MePPEP was likely the cause of larger intersubject variability of V_T for ^{11}C-MePPEP than for ^{18}F-FMPEP-d_2. The greater accuracy of the plasma concentration measurements of ^{18}F-FMPEP-d_2 was also reflected in the stability of V_T determined by increasingly truncating the plasma curve. Measurements from plasma attained at 90 min after injection were approximately as good for defining both the input function and the V_T as measurements from the entire 270 min of plasma data (Fig. 5B). We attribute this consistency between 90 and 270 min to the precision with which we were able to measure the input function, which in turn facilitated our precise measurements of V_T.

This retest analysis assumes that plasma clearance and receptor density in the brain were the same for both scans. The comparison of the 2 radioligands may be biased against ^{18}F-FMPEP-d_2, because the 2 scans for ^{11}C-MePPEP were done on the same day (morning and afternoon), whereas the interval between scans for ^{18}F-FMPEP-d_2 was 15–245 d. Although the retest variability of V_T was similar for both radioligands, ^{18}F-FMPEP-d_2 had a superior ICC, meaning that it is better able to distinguish between-subject from within-subject differences. Taken together, these data strongly suggest that the primary advantage of ^{18}F-FMPEP-d_2 over ^{11}C-MePPEP is the greater accuracy of the plasma measurements, which leads to greater accuracy of V_T and smaller sample sizes needed to detect differences between groups.

CONCLUSION

This initial evaluation of ^{18}F-FMPEP-d_2 in healthy human subjects showed that brain uptake and unchanged parent radioligand in plasma provide robust measurements of V_T, which is an index of receptor density. The scanning time should be no more than 120 min, because longer acquisitions are vulnerable to contamination of the brain with radiometabolites and spillover of radioactivity from the skull. Retest analysis shows that ^{18}F-FMPEP-d_2 has greater precision and accuracy than ^{11}C-MePPEP and will allow smaller sample sizes to detect significant differences between groups (e.g., patients vs. healthy subjects).

REFERENCES

1. Van Laere K. *In vivo* imaging of the endocannabinoid system: a novel window to a central modulatory mechanism in humans. *Eur J Nucl Med Mol Imaging.* 2007;34:1719–1726.
2. Terry GE, Liow JS, Zoghbi SS, et al. Quantitation of cannabinoid CB_1 receptors in healthy human brain using positron emission tomography and an inverse agonist radioligand. *Neuroimage.* 2009;48:362–370.
3. Donohue SR, Krushinski JH, Pike VW, et al. Synthesis, ex vivo evaluation, and radiolabeling of potent 1,5-diphenylpyrrolidin-2-one cannabinoid subtype-1 receptor ligands as candidates for in vivo imaging. *J Med Chem.* 2008;51:5833–5842.
4. Hashimoto K, Inoue O, Suzuki K, Yamasaki T, Kojima M. Deuterium isotope effect of $[^{11}C_1]N,N$-dimethylphenethyl-amine-α,α-d_2; reduction in metabolic trapping rate in brain. *Int J Rad Appl Instrum B.* 1986;13:79–80.
5. Schou M, Halldin C, Sovago J, et al. PET evaluation of novel radiofluorinated reboxetine analogs as norepinephrine transporter probes in the monkey brain. *Synapse.* 2004;53:57–67.
6. Yasuno F, Brown AK, Zoghbi SS, et al. The PET radioligand [^{11}C]MePPEP binds reversibly and with high specific signal to cannabinoid CB_1 receptors in nonhuman primate brain. *Neuropsychopharmacology.* 2008;33:259–269.
7. Zoghbi SS, Shetty HU, Ichise M, et al. PET imaging of the dopamine transporter with ^{18}F-FECNT: a polar radiometabolite confounds brain radioligand measurements. *J Nucl Med.* 2006;47:520–527.
8. Gandelman MS, Baldwin RM, Zoghbi SS, Zea-Ponce Y, Innis RB. Evaluation of ultrafiltration for the free-fraction determination of single photon emission computed tomography (SPECT) radiotracers: β-CIT, IBF, and iomazenil. *J Pharm Sci.* 1994;83:1014–1019.
9. Innis RB, Cunningham VJ, Delforge J, et al. Consensus nomenclature for in vivo imaging of reversibly binding radioligands. *J Cereb Blood Flow Metab.* 2007;27:1533–1539.
10. Burger C, Mikolajczyk K, Grodzki M, Rudnicki P, Szabatin M, Buck A. JAVA tools for quantitative post-processing of brain PET data [abstract]. *J Nucl Med.* 1998;39(suppl):277P.
11. Hawkins RA, Phelps ME, Huang S-C. Effects of temporal sampling, glucose metabolic rates, and disruptions of the blood-brain barrier on the FDG model with and without a vascular compartment: studies in human brain tumors with PET. *J Cereb Blood Flow Metab.* 1986;6:170–183.
12. Akaike H. A new look at the statistical model identification. *IEEE Trans Automat Contr.* 1974;19:716–723.
13. Fujita M, Imaizumi M, Zoghbi SS, et al. Kinetic analysis in healthy humans of a novel positron emission tomography radioligand to image the peripheral benzodiazepine receptor, a potential biomarker for inflammation. *Neuroimage.* 2008;40:43–52.

14. Carson RE, Huang SC, Green MV. Weighted integration method for local cerebral blood flow measurements with positron emission tomography. *J Cereb Blood Flow Metab.* 1986;6:245–258.

15. McGraw KO, Wong SP. Forming inferences about some intraclass correlation coefficients. *Psychol Methods.* 1996;1:30–46.

16. Abood ME, Ditto KE, Noel MA, Showalter VM, Tao Q. Isolation and expression of a mouse CB_1 cannabinoid receptor gene: comparison of binding properties with those of native CB_1 receptors in mouse brain and N18TG2 neuroblastoma cells. *Biochem Pharmacol.* 1997;53:207–214.

17. Glass M, Dragunow M, Faull RL. Cannabinoid receptors in the human brain: a detailed anatomical and quantitative autoradiographic study in the fetal, neonatal and adult human brain. *Neuroscience.* 1997;77:299–318.

18. Burns HD, Van Laere K, Sanabria-Bohorquez S, et al. [18F]MK-9470, a positron emission tomography (PET) tracer for *in vivo* human PET brain imaging of the cannabinoid-1 receptor. *Proc Natl Acad Sci USA.* 2007;104:9800–9805.

19. Van Laere K, Goffin K, Casteels C, et al. Gender-dependent increases with healthy aging of the human cerebral cannabinoid-type 1 receptor binding using [18F]MK-9470 PET. *Neuroimage.* 2008;39:1533–1541.